

Size-dependent modifications of the first-order Raman spectra of nanostructured rutile TiO₂

Varghese Swamy

Department of Materials Engineering, Monash University, Victoria 3800, Australia

(Received 15 December 2007; revised manuscript received 28 March 2008; published 13 May 2008)

The crystallite-size-dependent Raman spectral modifications observed for a suite of rutile TiO₂ nanocrystals are analyzed and compared to the characteristics of the Raman spectra that were reported for nanoscale rutile TiO₂ domains/crystallites embedded in thin films. The strong E_g and A_{1g} modes display disparate size dependencies in the various rutile nanostructures. The redshifts of the Raman frequencies, asymmetric peak broadening, and intensity/linewidth ratio reductions with decreasing crystallite size observed for nanopowder samples are consistent with phonon confinement. The nonsystematic Raman spectral modifications that are inconsistent with phonon confinement documented for the nanoscale rutile within thin films suggest that intrinsic crystallographic or extrinsic matrix influences can interfere and overprint the confinement effects.

DOI: [10.1103/PhysRevB.77.195414](https://doi.org/10.1103/PhysRevB.77.195414)

PACS number(s): 61.46.Df, 63.22.-m, 78.30.-j, 78.67.Bf

There has been an intense interest in the characterization of the size-dependent modifications of the first-order Raman spectra of TiO₂ phases, specifically that of anatase and rutile. The principal motivation for this research derives from the potential nanostructured anatase and rutile TiO₂ hold as promising materials for “energy” and “environmental” applications, with much of the current work focusing on their utilization in photocatalysis, photovoltaics, photochromics, electrochromics, and sensors.¹⁻³ It is hoped that the characterization of the size dependence of the Raman scattering and other physical properties, especially on nanodimensioned phases, could lead to the development of viable nondestructive size-estimation methods while also contributing to a better understanding of the unique behavior of these materials under finite-size regimes.

Nanostructured anatase is easily prepared in a range of sizes (with small dispersions), shapes, and forms (as nanocrystals, rods, tubes, wires, sheets, films, etc.) by using a variety of physical and chemical methods.^{1,3} This has allowed several detailed studies of the size dependence of its properties, including that of the phonon spectrum. Most efforts concentrated on the characterization of the size-dependent changes of the Raman frequency, linewidth (full width at half maximum), and intensity of the most intense $E_{g(1)}$ mode at ~ 144 cm⁻¹ of the nanoscale (ns) anatase (reviewed in Refs. 3–5). The anatase $E_{g(1)}$ band shows a systematic blueshift of the Raman frequency and peak broadening with the decreasing crystallite size. Among the suggested factors that contribute to the observed Raman spectral modifications in the ns-anatase, namely, phonon confinement, nonstoichiometry, and internal stress/surface tension effects, the confinement of phonons by finite-sized anatase crystallites has been posited as the most convincing proposal.³

In contrast to the broadly similar size-dependent modifications of the anatase Raman spectra reported in various studies (albeit with disagreements in regard to their origin), the relatively limited number of investigations on ns-rutile have produced vastly different and, in some instances, contradictory results concerning the size-dependent Raman spectral modifications.⁶⁻¹² In this paper, we suggest that the disparate results, especially well documented for the size dependencies of the most pronounced E_g and A_{1g} modes (at 447 and 612 cm⁻¹ for coarse-grained samples), stem from

the intrinsic nature of the materials examined in various studies.

The grain-size effects contributing to the modifications of the first-order rutile Raman spectrum was suggested in a hydrothermal synthesis study involving a limited number of nanocrystalline samples.⁹ A more detailed analysis of the size-dependent modifications of the rutile Raman spectra, including a comparison to the most completely investigated Raman spectra of a rutile-structured nanocrystalline oxide, which is of rutile SnO₂, suggested distinct size-dependent changes for the E_g and A_{1g} modes (redshifts, line broadening, and intensity/linewidth ratio) that are consistent with a phonon confinement behavior.¹⁰

The Raman spectra of compacted nanocrystalline rutile-anatase mixtures, which were produced via gas condensation of Ti and its subsequent oxidation (with or without thermal annealing), were investigated by Siegel and co-workers.⁶⁻⁸ The broadening and frequency shifts of the rutile E_g (at 418 ± 10 or 424 cm⁻¹) and A_{1g} modes (at 600 ± 7 or 612 cm⁻¹) were interpreted to reflect intracrystalline defects and oxygen nonstoichiometry (a dependence on internal stress or the grain size was ruled out).

The latest Raman studies on ns-rutile prepared through the physical route also revealed contrasting modifications to the E_g and A_{1g} modes.^{11,12} Nanocrystalline rutile-anatase mixtures within cluster-assembled TiO₂ thin films deposited on Si and Al₂O₃ substrates showed redshifts for the E_g mode and random shifts for the A_{1g} mode.¹¹ Nonstoichiometry effects, which are common to materials prepared by using physical methods, was ruled out as the reason for the spectral changes. According to the authors, the modifications of the E_g mode fairly agreed with a phonon confinement model (PCM) prediction, but that of the A_{1g} mode did not. The authors suggested that the dielectric constant of the embedding medium influences the Raman spectral modifications in the nanostructured phase.¹¹

The Raman scattering by “nanomosaic” rutile in a single layer TiO₂ and TiO₂-Al₂O₃ nanolaminate film rf-sputter deposited on a Au-coated glass or a fused silica revealed bulk-like Raman shifts for the E_g mode while the A_{1g} mode was significantly blueshifted¹²—a behavior not reported for any other ns-rutile Raman spectra. The blueshift of the A_{1g} mode was attributed to an apical Ti-O bond shortening in the TiO₆

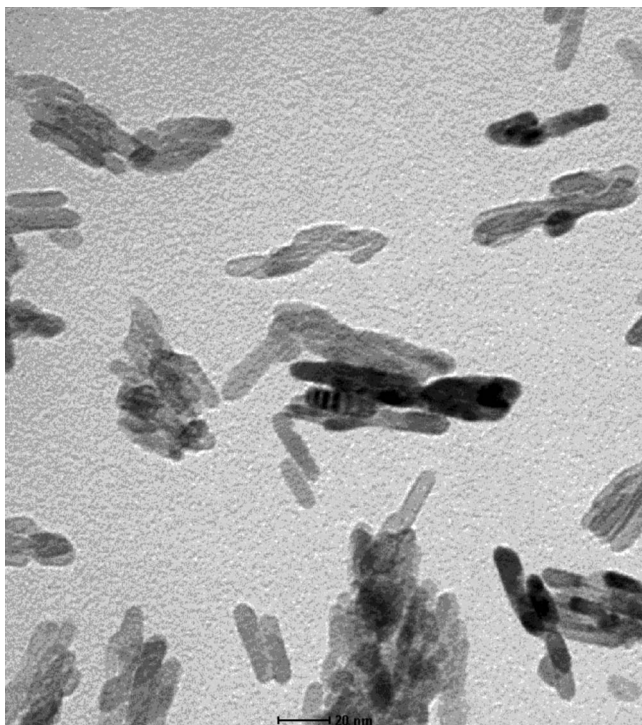


FIG. 1. Transmission electron micrograph of a nanocrystalline rutile sample. The large anisotropy in the crystallite morphology (elongated prismatic crystallites with aspect ratios $\sim 1:3-1:5$) contributes to a significant uncertainty in the Scherrer size estimates [the (110) reflection gives a value ~ 9 nm, whereas the majority of the crystallites measure $\sim 4-5 \times 15-20$ nm in the TEM].

octahedral unit of the rutile crystal structure.¹²

With the objective of reconciling the contrasting Raman scattering data reported for ns-rutile TiO_2 and to assess phonon confinement as a plausible explanation for at least some of the observed behaviors, we reexamined the Raman spectra of the nanocrystalline rutile TiO_2 synthesized by using the hydrothermal (HT) method.^{9,10,13} The HT method has been documented to yield strain-free, stoichiometric nanorutile crystallites with a small size dispersion.¹³ For the HT synthesis, TiCl_4 was added to a cold distilled water while under constant stirring. The aqueous solution thus obtained was filtered and aliquots were transferred to autoclaves and kept at fixed temperatures in the range of 120–220 °C for 2–3 h. The product (suspension) was filtered, washed, and dried at 80 °C. The x-ray diffraction (conventional¹⁰ and unpublished angle-dispersive synchrotron) data obtained on the samples suggested a phase-pure rutile and the transmission electron micrographs showed elongated prismatic crystals (Fig. 1).

The unpolarized Raman spectra were recorded on seven nanocrystalline rutile (powder) samples and on commercial microparticle rutile, rutile+anatase (Alpha), and anatase (Aldrich) powders by using a Dilor spectrometer. The Raman scattering was excited with a 514.5 nm Ar^+ ion laser in the backscattering geometry. The average crystallite sizes estimated by using the Scherrer method with the (110) x-ray diffraction peak for the nanocrystalline samples were 5.0, 6.7, 7.1, 8.8, 14.7, 19.1, and 23.8 nm. A minimum of six

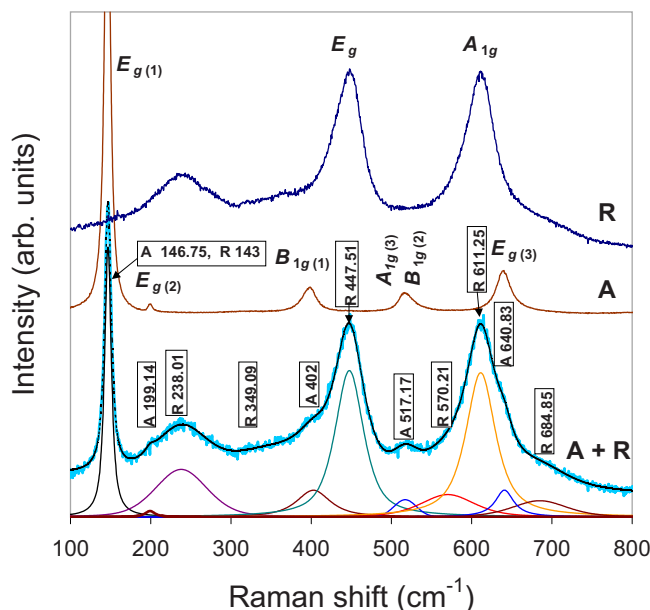


FIG. 2. (Color online) As-recorded (uncorrected for peak positions) Raman spectra of the microparticle rutile (labeled R), anatase (A), and a rutile+anatase mixture (A+R). The dominant first-order Raman peaks of rutile and anatase are marked. The numbers in the boxes correspond to the peak positions (Raman shifts) obtained in a multipeak fit for the anatase-rutile Raman spectra (peaks at the bottom).

Raman spectra were analyzed for each sample and the averages of best fits are reported here. The as-recorded digital spectra were fitted by using combinations of the Gaussian and the Lorentzian functions to obtain Raman wave numbers and linewidths in a multipeak fitting procedure by employing the Gaussian deconvolution method. Here, we evaluate the size dependencies experimentally obtained for the Raman wave numbers and peak widths of the two dominant rutile modes, namely E_g and A_{1g} , against those that were calculated by using a recent PCM.¹¹ The PCM was formulated by using inelastic neutron scattering data¹⁴ and intrinsic linewidths measured for microcrystalline powder samples as inputs.

It should be emphasized that the analysis of the crystallite-size-related changes in the Raman shifts, peak broadening, and peak asymmetry is best done on the Raman spectra that were recorded for a suite of phase-pure samples with varying average crystallite sizes. As seen in Fig. 2, while extracting the Raman peak positions and linewidths for the rutile E_g and A_{1g} modes from the spectra of a rutile-anatase mixture, the contributions that are due to the B_{1g} , A_{1g} , and E_g anatase modes (flanking the rutile E_g and A_{1g} modes), as well as that due to the “background” (presumably resulting from second-order phonon processes of the rutile Raman spectrum¹⁰), need to be subtracted from the overall peak profile. The deconvoluted values are very sensitive to the fitting procedure; our analyses suggested an extreme sensitivity to the fitting procedure, especially at very small sizes (see below), even for the Raman spectra recorded for the phase-pure rutile nanocrystals. In particular, the errors in the peak width increase for the smaller crystallites because the combinations of the Gaussian and the Lorentzian functions

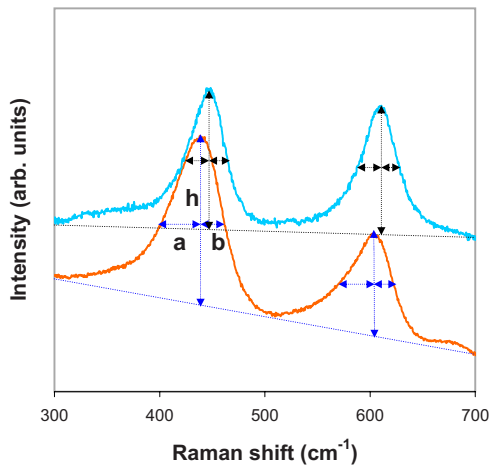


FIG. 3. (Color online) Part of the Raman spectra of 5.0 nm (lower) and 23.8 nm (upper) rutile showing an increased peak asymmetry (increased a/b ratio) and a reduced intensity/peakwidth ratio $[h/(a+b)]$ with a decreasing crystallite size for the E_g and A_{1g} modes.

are not entirely adequate at smaller crystallite sizes owing to the increased asymmetry and broadening (Fig. 3). The size-dependent redshift, peak broadening, and intensity/peakwidth ratio reduction are clearly seen in Fig. 3 and are

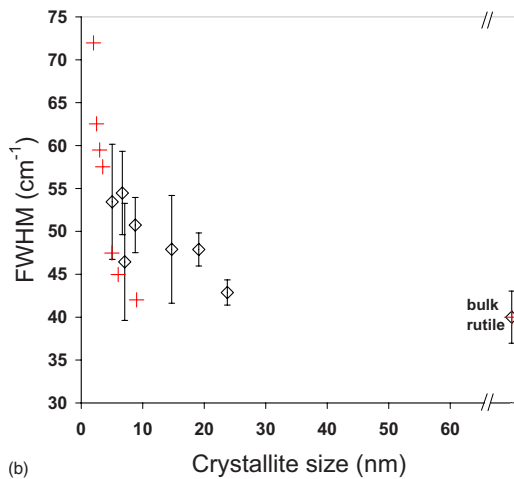
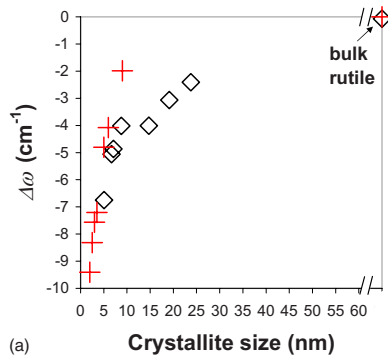


FIG. 4. (Color online) Crystallite size-dependent variations in the relative Raman frequencies (a) and linewidths (b) for the A_{1g} rutile Raman mode. Diamonds—experimental data; plus sign—phonon confinement prediction (Ref. 11).

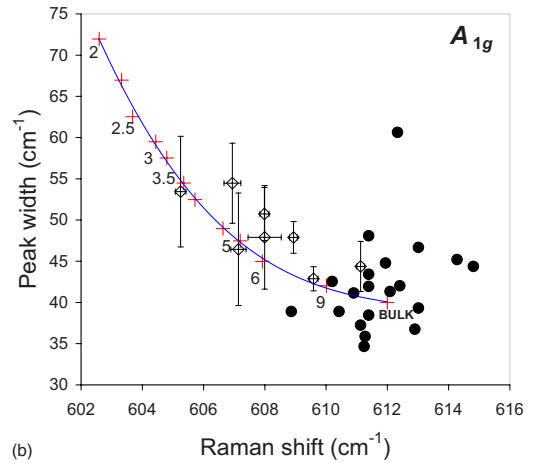
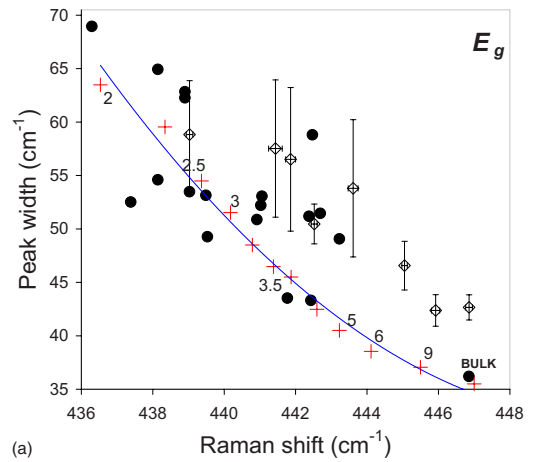


FIG. 5. (Color online) Raman shift vs peak width correlations for the E_g (a) and A_{1g} (b) modes of rutile TiO_2 . The curves are fits to the PCM-predicted data (plus signs) (Ref. 11); the solid circles represent the experimental data from Ref. 11; and the open diamonds with error bars represent the data from this study.

consistent with the known phonon dispersion relations.¹⁰

In Fig. 4, the experimental and PCM-predicted crystallite-size-dependent variations in the relative Raman shifts and peak widths for the A_{1g} mode are compared. It is to be noted that the data in Fig. 4(a) are slightly different to that in Ref. 10 because the present data represent the analysis of several spectra. It was noted that the PCM is applicable for rutile SnO_2 with crystallite sizes $>10\text{--}15$ nm.^{15,16} For smaller crystallite sizes, not only do the PCM-calculated Raman spectra display an exaggerated asymmetry but increasing disagreement may also be related to factors such as crystallite size dispersion, intracrystalline defects, or disordered regions within the crystallites.¹⁵ For the rutile TiO_2 nanocrystals, however, the experimentally measured and PCM-predicted size-dependent variations are only in semiquantitative agreement (Fig. 4).

A correlation between the Raman shifts and linewidths with varying crystallite sizes has been established for a variety of nanocrystalline materials.^{4,11,17–21} This correlation is perhaps more useful^{11,22} than the crystallite size vs Raman shift/linewidth correlations, especially in the case of rutile nanocrystals possessing high aspect ratios such as TiO_2

(Refs. 10 and 13) and RuO_2 ,²³ for which the Scherrer size estimates may be compromised by the large anisotropy in the crystallite morphology (Fig. 1). In Fig. 5, the Raman shift vs linewidth data obtained in this work for the E_g and A_{1g} modes are superimposed on the correlations obtained by using the PCM.¹¹ For the E_g mode, the agreement between the PCM-values and the experimental data obtained from different regions of the thin-film samples [represented by the solid circles in Fig. 5(a)] was considered *reasonable* in the earlier study.¹¹ The present data, which are represented by the open diamonds in Fig. 5(a), show a somewhat systematic overestimation of the linewidths in relation to the PCM prediction. In part, it may be due to the instrumental broadening not explicitly accounted for here. However, a weak tendency of the linewidth overestimation is also seen in the earlier experimental data.¹¹ This seems to suggest that the PCM provides only a semiquantitative prediction of this mode.

In the case of the A_{1g} mode, in contrast to the E_g mode, total disagreement was obtained in the previous study¹¹ between the PCM-predicted and the experimental Raman shift-peak width correlations, which are represented in Fig. 5(b) by the plus signs and solid circles, respectively. The PCM was fitted with the same confinement function for both the E_g and the A_{1g} modes and, therefore, was expected to give similar predictions. The disagreement obtained for the A_{1g} mode was interpreted by the authors as a failure of the PCM.^{11,24} As can be seen in Fig. 5(b), unlike their data (obtained from the embedded ns-rutile in thin-film samples) that straddle the “bulk” end of the correlation, the present data are aligned along the PCM-predicted trend, suggesting that for nano-

powder samples wherein three-dimensional confinement effects are practically unhindered by the influences of the surrounding medium, the PCM also gives a reasonable prediction for this mode.

Although the PCM has been applied with varying degrees of success to a range of materials²² and provides very valuable information on typical size ranges depending on the material,²⁵ its success must be gauged against the fact that it is only a phenomenological model devised to describe the relaxation of the $q \approx 0$ phonon momentum selection rule.^{17,22} A number of assumptions and known shortcomings (see Ref. 25) embody the PCM, including the assumption of propagating phonons (bulk dispersion curves) to describe confined modes, uniform particle size distribution, and choice of a particular confinement function. The nonideal phonon-related aspects of real nanomaterials (such as nonuniform particle size distribution, chemical defects, crystallite imperfections, grain boundaries and interfaces, phonon interactions with other nanoparticles or matrix, and existence of surface modes) are bound to complicate the picture.

In summary, phonon confinement, crystallite-matrix interactions (not fully characterized as yet), and crystal structure characteristics all contribute to the divergent modifications observed in the first-order Raman spectra of stoichiometric ns-rutile TiO_2 . The PCM gives a semiquantitative prediction of the Raman spectra (at least in a certain crystallite size range) of rutile TiO_2 nanocrystals, as with ns-rutile SnO_2 (Refs. 15 and 16) and RuO_2 .²³ Structural peculiarities¹² or crystallite-matrix couplings (when embedded)¹¹ can lead to remarkably different phonon behaviors that obscure the confinement effects.

-
- ¹U. Diebold, Surf. Sci. Rep. **48**, 53 (2003).
²O. Carp, C. L. Huisman, and A. Reller, Prog. Solid State Chem. **32**, 33 (2004).
³X. Chen and S. S. Mao, Chem. Rev. (Washington, D.C.) **107**, 2891 (2007).
⁴V. Swamy, A. Kuznetsov, L. S. Dubrovinsky, R. A. Caruso, D. G. Shchukin, and B. C. Muddle, Phys. Rev. B **71**, 184302 (2005).
⁵M. J. Šćepanović, M. Grujić-Brojčin, Z. D. Dohčević-Mitrovoć, and Z. V. Popović, Appl. Phys. A: Mater. Sci. Process. **86**, 365 (2007).
⁶C. A. Melendres, A. Narayanasamy, V. A. Maroni, and R. W. Siegel, J. Mater. Res. **4**, 1246 (1989).
⁷J. C. Parker and R. W. Siegel, J. Mater. Res. **5**, 1246 (1990).
⁸J. C. Parker and R. W. Siegel, Appl. Phys. Lett. **57**, 943 (1990).
⁹H. Cheng, J. Ma, Z. Zhao, and L. Qi, Chem. Mater. **7**, 663 (1995).
¹⁰V. Swamy, B. C. Muddle, and Q. Dai, Appl. Phys. Lett. **89**, 163118 (2006).
¹¹T. Mazza, E. Barborini, P. Piseri, P. Milani, D. Cattaneo, A. Li Bassi, C. E. Bottani, and C. Ducati, Phys. Rev. B **75**, 045416 (2007).
¹²C. R. Aita, Appl. Phys. Lett. **90**, 213112 (2007).
¹³G. Li, L. Li, J. Boerio-Goates, and B. F. Woodfield, J. Mater. Res. **18**, 2664 (2003).
¹⁴J. G. Traylor, H. G. Smith, R. M. Nicklow, and M. K. Wilkinson, Phys. Rev. B **3**, 3457 (1971).
¹⁵A. Diéguez, A. Romano-Rodríguez, A. Vilà, and J. R. Morante, J. Appl. Phys. **90**, 1550 (2001).
¹⁶M. Fernandez-Garcia, A. Martinez-Arias, J. C. Hanson, and J. A. Rodriguez, Chem. Rev. (Washington, D.C.) **104**, 4063 (2004).
¹⁷H. Richter, Z. P. Wang, and L. Ley, Solid State Commun. **39**, 625 (1981).
¹⁸R. J. Nemanich, S. A. Solin, and R. M. Martin, Phys. Rev. B **23**, 6348 (1981).
¹⁹K. K. Tiong, P. M. Amirtharaj, F. H. Pollak, and D. E. Aspnes, Appl. Phys. Lett. **44**, 122 (1984).
²⁰C. J. Doss and R. Zallen, Phys. Rev. B **48**, 15626 (1993).
²¹W. S. O. Rodden, C. M. Sotomayor Torres, and C. N. Ironside, Semicond. Sci. Technol. **10**, 807 (1995).
²²A. K. Arora, M. Rajalakshmi, T. R. Ravindran, and V. Sivasubramanian, J. Raman Spectrosc. **38**, 604 (2007).
²³C. L. Cheng, Y. F. Chen, R. S. Chen, and Y. S. Huang, Appl. Phys. Lett. **86**, 103104 (2005).
²⁴T. Mazza and P. Milani, Appl. Phys. Lett. **91**, 046103 (2007).
²⁵G. Gouadec and P. Colomban, Prog. Cryst. Growth Charact. Mater. **53**, 1 (2007).